nature communications

Article

https://doi.org/10.1038/s41467-024-54846-2

Future land carbon removals in China consistent with national inventory

Received: 31 May 2024

Accepted: 21 November 2024

Published online: 30 November 2024

Check for updates

Yue He[1,2], Shilong Piao[1] ✉, Philippe Ciais[3], Hao Xu[1] & Thomas Gasser[2] ✉

China's commitment to carbon neutrality by 2060 relies on the Land Use, Land-Use Change, and Forestry (LULUCF) sector, with forestation targets designed to enhance carbon removal. However, the exact sequestration potential of these initiatives remains uncertain due to differing accounting conventions between national inventories and scientific assessments. Here, we reconcile both estimates and reassess LULUCF carbon fluxes up to 2100, using a spatially explicit bookkeeping model, state-of-the-art historical data, and national forestation targets. We simulate a carbon sink of −0.24 ± 0.03 Gt C yr^{-1} over 1994–2018 from past forestation efforts, aligned well with the national inventory. Should the official forestation targets be followed and extended, this could reach −0.35 ± 0.04 Gt C yr^{-1} in 2060, offsetting 43 ± 4% of anticipated residual fossil CO_2 emissions. Our findings confirm the key role of LULUCF in carbon sequestration, but its potential will decline if forestation efforts cease, highlighting the necessity for emission reductions in other sectors to achieve carbon neutrality.

China has pledged to become carbon neutral by 2060 as part of its Nationally Determined Contribution (NDC) under the Paris Agreement[1,2]. Central to this pledge is the concept of carbon neutrality, which involves achieving a balance between all anthropogenic CO_2 emissions and the removal of CO_2 from the atmosphere by land, ocean, and human activities[3,4]. Recognizing the dual role of land—both as a source of emissions and a vital avenue for carbon capture—is crucial in this context. This understanding underscores the importance of carbon removal through Land Use, Land-Use Change, and Forestry (LULUCF) sector in offsetting emissions that are hard to abate[4,5]. Although China has established several policy targets for afforestation and reforestation (collectively referred to as forestation; Supplementary Table 1), their carbon removal potential remains largely unquantified. Since the 1980s, China has launched extensive forestation projects, increasing forest coverage from 157 million hectares (Mha) in 1990 to 220 Mha in 2020[6–9]. Understanding these historical dynamics is key to projecting reliable and consistent carbon removal potential from LULUCF in the future and to facilitating progress tracking toward China's carbon neutrality goal.

Accurate quantification of anthropogenic LULUCF carbon fluxes remains fraught with large uncertainties[10–16]. One key discrepancy arises from the misalignment in definitions between global models and national greenhouse gas inventories (NGHGIs) (Supplementary Fig. 1). In model-based studies, only carbon fluxes from direct anthropogenic activities (e.g., land-use changes, wood harvest, and subsequent regrowth) are categorized as LULUCF (noted E_{LUC})[9,17–20], while the indirect effects due to environmental changes (e.g., climate change and CO_2 fertilization) are not considered anthropogenic (noted S_{LAND}). In contrast, partly due to the near-impossibility of separating direct and indirect effects in practice (as only the sum, noted F_{NET}, can be physically observed), NGHGIs consider all carbon fluxes occurring on managed land as LULUCF (noted $F_{NET(man)}$)[13,14,21]. Comparison of LULUCF fluxes over 1994–2018 following both definitions reveal a substantial gap in China: while the NGHGI reports a sink of −0.23 gigatons of carbon per year (Gt C yr^{-1}), the Global Carbon Budget (GCB), based on the average of three bookkeeping models (i.e., OSCAR-GCB, BLUE and H&C), indicates a source of 0.01 Gt C yr^{-1} (Fig. 1).

[1]Institute of Carbon Neutrality, Sino-French Institute for Earth System Science, College of Urban and Environmental Sciences, Peking University, Beijing, China. [2]International Institute for Applied Systems Analysis (IIASA), Laxenburg, Austria. [3]Laboratoire des Sciences du Climat et de l'Environnement (LSCE), CEA CNRS UVSQ, 91191 Gif Sur Yvette, France. ✉e-mail: slpiao@pku.edu.cn; gasser@iiasa.ac.at

https://doi.org/10.1038/s41467-024-54846-2

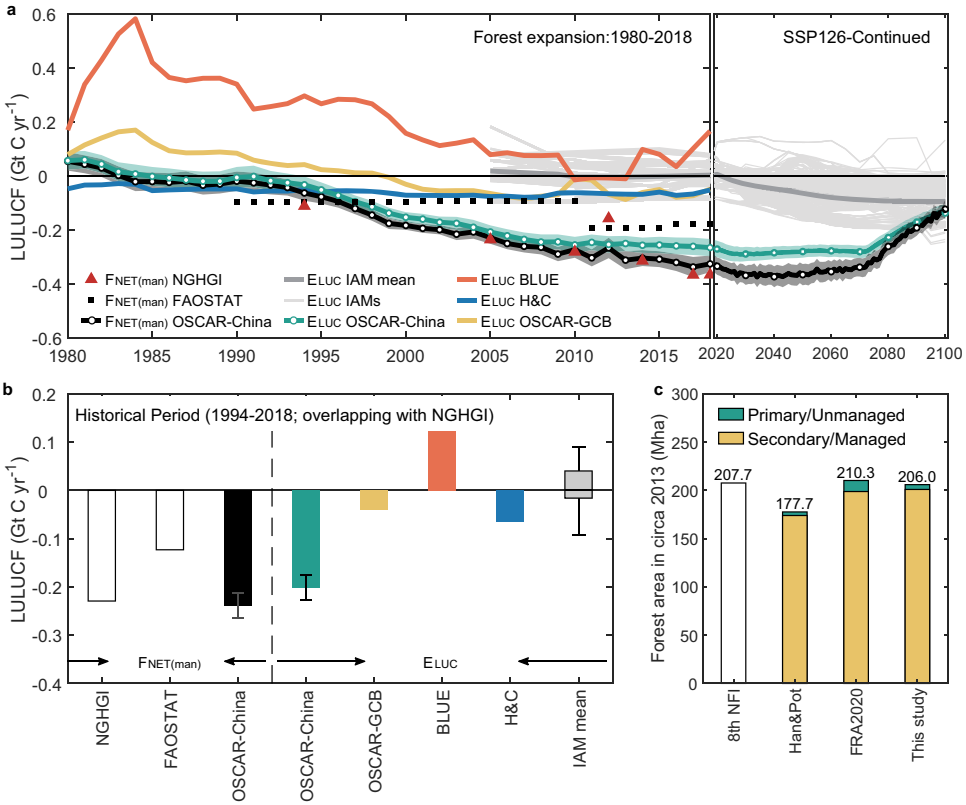

Fig. 1 | Comparison of anthropogenic carbon fluxes from Land Use, Land-Use Change, and Forestry (LULUCF) estimated by different methods. The values are defined from an atmospheric perspective: positive values indicate emissions and negative ones represent removals. **a** Annual anthropogenic carbon fluxes from LULUCF since 1980. The green line with circular markers represents LULUCF fluxes considering only the impact of direct effects (E_{LUC}) simulated by OSCAR-China. This is compared with E_{LUC} deduced from OSCAR-GCB (yellow line), BLUE (orange line) and H&C (blue line). E_{LUC} estimates from individual IAMs (thin gray lines) and the IAM mean (thick gray line) are also shown. The black line with circular markers represents LULUCF fluxes considering both direct and indirect effects on managed land ($F_{NET(man)}$) simulated by OSCAR-China, to facilitate a conceptual comparison with NGHGI (black triangles) and FAOSTAT (black squares). Note that the carbon emissions from peat burning and drainage are not considered and were removed from the datasets if originally included. **b** Multi-year mean LULUCF fluxes over the period of 1994–2018. The uncertainty bars of OSCAR-China E_{LUC} and $F_{NET(man)}$ denote the weighted standard deviation from a constrained Monte Carlo ensemble of 1000 elements, while the box plot for IAMs displays the median and interquartile range. **c** Forest area estimates based on various data sources. From left to right: (1) the 8th National Forest Inventory (NFI) in China; (2) the forest map used by Grassi et al.[48], which integrates forest cover data from Hansen et al.[63] and non-intact forest data from Potapov et al.[64] for 2013 (Han&Pot); (3) the Global Forest Resources Assessment 2020 (FRA2020); and (4) the reconstructed forest map used in this study. While the terms "unmanaged" and "managed" broadly correspond to "primary" and "secondary", their exact definitions vary depending on the dataset.

Another key source of discrepancy is the land-use change forcing data used to drive the models. In particular, the widely used Land-Use Harmonization dataset (LUH2) fails to capture the observed increase in forest area in China documented by the Food and Agriculture Organization (FAO) data, yet this increase has been noted in previous studies[9,22]. While biogeochemical parameters also add a layer of uncertainty, a previous model-based study suggests that it is primarily the land-use change data that drives the uncertainties in E_{LUC} in China[12]. Lastly, a key limitation in many observation-based studies is their focus on the impact of forestation on forest biomass sinks alone, often using age-biomass relationships to estimate carbon sequestration[23–29]. While these empirical statistical models provide useful insights into forest biomass sinks, they do not account for the broader LULUCF sector's contribution, nor can they be directly aligned with national inventory estimates of carbon sinks in the LULUCF sector. Consequently, there is a noticeable gap in the evaluation of LULUCF carbon dynamics in China that aligns with the NGHGI convention, encompassing both historical periods and future projections.

To consider these issues, we have implemented OSCAR-China, a refined 0.5° × 0.5° gridded version of the reduced-complexity model OSCAR, specifically tailored for China (Methods). Of the three bookkeeping models used in the GCB annual exercise, OSCAR distinguishes itself by incorporating biogeochemical processes that enable simulating all aspects of the land carbon cycle under environmental and land-use changes[11,12] and bridge the gap in definitions[13]. OSCAR-China inherits this feature and incorporates spatially explicit, observation-based historical land-use change data[9].

Our analysis begins with an assessment of historical carbon emissions and removals by LULUCF in China from 1900 to 2018, using NGHGI as a benchmark. We then explore future carbon removal scenarios up to 2100 in alignment with national forestation targets (Supplementary Table 1), considering different projections of climate change, with a specific focus on the role of LULUCF in achieving China's 2060 carbon neutrality target. To address uncertainties in our projections, we examine various spatial strategies for forestation and consider the impact of different wood harvesting management practices on carbon sequestration potential. Through this comprehensive approach, we aim to provide more robust estimates of the LULUCF sector's potential contribution to carbon neutrality in China.

Results

Historical LULUCF fluxes in China

To address biogeochemical uncertainty, we run a series of 1000 Monte Carlo simulations constrained by observation-based forest vegetation

https://doi.org/10.1038/s41467-024-54846-2

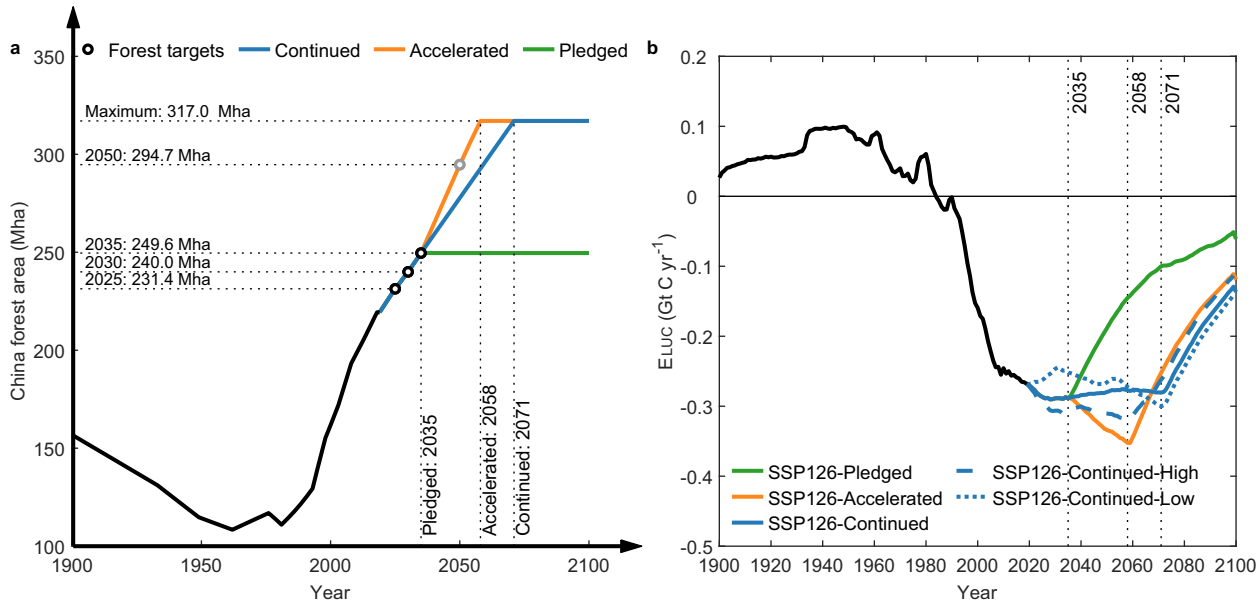

Fig. 2 | Forest expansion trajectories and corresponding carbon removal dynamics by direct effects. a Historical forest area changes and future forest expansion trajectories. The black circles indicate three official policy targets, while the gray circle denotes the non-official target (see Supplementary Table 1 for details). **b** Direct carbon removals (E_{LUC}) under these different forest expansion trajectories. Dashed and dotted lines show different spatial allocation strategies for the corresponding trajectory (Methods). Uncertainty ranges are not shown for legibility.

carbon stock data from the 9th National Forest Inventory (NFI) and the assessed net terrestrial carbon sink from the latest Regional Carbon Cycle Assessment and Processes report (RECCAP2) initiative[30,31] (see Methods). Our model demonstrates good performance in capturing both temporal and spatial dynamics of forest carbon in China, aligning well with independent observations (Supplementary Fig. 2).

To ensure definitional alignment with NGHGI, we calculate $F_{NET(man)}$ by combining the simulated direct effects (E_{LUC}) with the indirect effects on managed land ($S_{LAND(man)}$). The latter involves multiplying the simulated S_{LAND} in forests by the fraction of managed forests[14]. Our model simulates a substantial shift in $F_{NET(man)}$ from 1980 to 2018, transitioning from a net carbon emission (0.04 ± 0.03 Gt C yr^{-1}; weighted average and standard deviation) to a net carbon removal (-0.33 ± 0.03 Gt C yr^{-1}), demonstrating the impact of China's forestation policies (Fig. 1). Our simulations align well with the NGHGI data in the overlapping period of 1994–2018, simulating -0.24 ± 0.03 Gt C yr^{-1} against a reported -0.23 Gt C yr^{-1}. This alignment shows the consistency and reliability of our simulation based on the NGHGI definition. Our data on total forest area (of which 95% is assumed managed, see Methods) also shows strong agreement with the national inventory (Fig. 1c).

Under the usual definition used in scientific assessments, our E_{LUC} are a notable carbon sink, with an average of -0.20 ± 0.03 Gt C yr^{-1} over 1994–2018 (Fig. 1). This markedly diverges from the results of the GCB, which are based on three bookkeeping models: BLUE[20], H&C[22], and a country-level version of OSCAR driven with different data (OSCAR-GCB[12]). Specifically, BLUE, utilizing the LUH2 dataset, suggests a significant source due to deforestation (0.12 Gt C yr^{-1}), whereas H&C, utilizing the FAO data, shows a sink (-0.07 Gt C yr^{-1}), reflecting increased forestation. OSCAR-GCB, integrating both datasets, presents a weaker sink of -0.04 Gt C yr^{-1}. While differences in the chosen land-use change datasets significantly contribute to these disparities, variances in model assumptions can also exert influence[10]. Moreover, when comparing our E_{LUC} estimates with Integrated Assessment Models (IAMs) sourced from the AR6 scenario database (Methods), the IAMs fail to capture the current levels of carbon removal from LULUCF (Fig. 1), which casts doubts on their projected mitigation pathways for this sector in China.

Potential carbon removal from LULUCF

Building upon the validated OSCAR-China model, we project the magnitude and temporal evolution of LULUCF fluxes up to the end of this century, in line with national targets for forest coverage. To this end, we have developed three land-use change scenarios based on varying assumptions regarding policy continuity in forest area expansion after achieving all official targets by 2035. These include continued forestation, which maintains forestation efforts after 2035; accelerated forestation, which increases efforts to meet a more ambitious, non-official target set for 2050; and pledged forestation, which halts efforts after 2035, thereby solely fulfilling official targets (Fig. 2a). All scenarios are constrained by the land area suitable for forestation in China, capped at a maximum potential of 317 Mha (Methods). By default, we also assume new forests will remain largely unexploited, with reduced wood harvest in the future following SSP1-2.6. These land-use change scenarios are then combined with three climate change scenarios (SSP1-2.6, SSP2-4.5, and SSP5-8.5), resulting in a total of nine combinations. Of these, we primarily focus on the SSP126-Continued scenario, which is more closely aligned with China's carbon neutrality goal.

Under a continued forestation effort, E_{LUC} could provide a steady carbon removal until the 2060s with an annual average of -0.28 ± 0.02 Gt C yr^{-1} over 2055–2065 (Table 1). This continuous removal is the result of the roughly linear expansion of forest areas and would last only until ~2040 should forestation be limited to the pledged 2035 target (Fig. 2b). Projections then show a decline in carbon removal as of ~2070 even in the continued case, as forestation reaches maximum area availability, eventually falling to -0.14 ± 0.02 Gt C yr^{-1} in 2100. In a scenario of accelerated forestation, carbon removals would first increase and culminate at -0.35 ± 0.03 Gt C yr^{-1} ~2060 and then steadily decrease in a similar fashion after having reached the maximum area availability. Note that because E_{LUC} is the component of the land carbon flux that describes

Table 1 | Synthesis of the Land Use, Land-Use Change, and Forestry (LULUCF) carbon fluxes across land-use change scenarios with a detailed breakdown by key land-use change activities and processes

SSP1-2.6	Continued	Accelerated	Pledged
	Cumulative carbon removal by direct effects during 2019–2100 (Gt C)		
Default spatial allocation strategy	−20.6 ± 1.7	−21.1 ± 1.8	−13.5 ± 1.5
High-carbon density priority (high)	−20.9 ± 1.8	−21.2 ± 1.8	−14.7 ± 2.0
Low-carbon density priority (low)	−20.1 ± 1.6	−20.8 ± 1.7	−11.8 ± 1.3
	Cumulative carbon removal by direct effects during 2019–2100 (Gt C)		
Deforestation	1.5 ± 0.3	1.5 ± 0.3	1.5 ± 0.3
Other land-use transitions	−0.9 ± 0.8	−0.9 ± 0.9	−0.9 ± 0.8
Forestation and wood harvest	−21.2 ± 1.7	−21.6 ± 1.8	−14.0 ± 1.3
	Cumulative carbon removal from LULUCF during 2019–2100 (Gt C)		
Direct effects (E_{LUC})	−20.6 ± 1.7	−21.1 ± 1.8	−13.5 ± 1.5
Indirect effects ($S_{LAND(man)}$)	−4.8 ± 1.8	−4.9 ± 1.8	−4.2 ± 1.6
Total ($F_{NET(man)}$)	−25.4 ± 2.4	−26.0 ± 2.5	−17.7 ± 2.0
	Carbon removal from LULUCF in 2060 (Gt C yr^{-1}) *		
Direct effects (E_{LUC})	−0.28 ± 0.02	−0.33 ± 0.03	−0.14 ± 0.02
Indirect effects ($S_{LAND(man)}$)	−0.07 ± 0.03	−0.08 ± 0.03	−0.06 ± 0.02
Total ($F_{NET(man)}$)	−0.35 ± 0.04	−0.41 ± 0.04	−0.20 ± 0.03
	Contribution of LULUCF in offsetting hard-to-abate emissions in 2060		
Direct effects (E_{LUC})	33.8 ± 2.7%	40.8 ± 3.1%	16.9 ± 2.5%
Indirect effects ($S_{LAND(man)}$)	8.9 ± 3.3%	9.5 ± 3.6%	7.3 ± 2.7%
Total ($F_{NET(man)}$)	42.6 ± 4.5%	50.3 ± 5.0%	24.2 ± 3.8%

*We approximate 2060 using the average value from 2055 to 2065 to reduce the uncertainties from interannual variability in S_{LAND}.
Focus is on three land-use change scenarios: continued, accelerated and pledged forestation, combined with the SSP1-2.6 climate change scenario, with default spatial allocation strategy except where explicitly stated (Methods). The first two segments represent only the direct effects from LULUCF (E_{LUC}), while the subsequent segments display both direct and indirect effects, as well as, the total effects from LULUCF. Positive values represent emissions, while negative values indicate removals.

the direct effects of human activities, it is only marginally impacted by the climate change scenario (Fig. 3a).

Looking in more detail at different carbon pools under the continued forestation scenario, E_{LUC} is dominated by vegetation regrowth, supplemented by a delayed response of soil systems, and partially offset by the oxidation of harvested wood products (Fig. 3b). Spatial analysis suggests that over 2019–2100, the majority of carbon removal will occur in the precipitation-rich regions of southern and southwestern China, while emissions are mainly expected in the south, southwest, and northeast China, due to historical deforestation and other land-use changes (Fig. 4a–c). The future carbon emissions attributable to historical deforestation are largely a legacy effect caused by the inertia of biogeochemical processes such as the decomposition of residual biomass and the equilibration of carbon in soils.

The indirect effects of human activities on the land carbon sink excluding direct land use (S_{LAND}) show a strong increase in removal until mid-century, after which point the response depends markedly on the assumed climate change scenario (Fig. 3c). In SSP5-8.5, it keeps increasing, whereas, in SSP2-4.5 and SSP1-2.6, it decreases in intensity to an estimated carbon flux of 0.01 ± 0.02 Gt C yr^{-1} in 2100 under the latter scenario. These changes in S_{LAND} broadly follow the scenarios' changes in atmospheric CO_2, as CO_2 fertilization in OSCAR is significant and above the average of models from the Coupled Model Intercomparison Project Phase 6 (CMIP6)[32], although this effect remains modulated by climate-carbon feedbacks[4,33].

It follows that under the SSP1-2.6-Continued scenario, indirect effects contribute 18 ± 6% of the NGHGI-compatible carbon removals ($F_{NET(man)}$) over 2019–2100, markedly less than the 82 ± 6% from direct effects (Fig. 4d–f). The contributions of indirect effects are notably higher under SSP2-4.5 and SSP5-8.5, at 27 ± 9% and 39 ± 11%, respectively. This contribution is expected to vary as S_{LAND} responds to atmospheric CO_2 and climate change, with a marked decrease of the indirect effects under SSP1-2.6 (Figs. 3 and Supplementary Fig. 3). Including indirect effects in the national accounting of carbon removals therefore creates a moving target in LULUCF mitigation strategies: one influenced by the global climate pathway that humanity will follow and that may mask actual mitigation efforts because of opposite evolutions in the direct and indirect land carbon fluxes[13].

LULUCF contribution to 2060 carbon neutrality

Achieving carbon neutrality in 2060 requires reducing Chinese emissions by 7–8 Gt CO_2 per year, primarily through energy and industrial transformations, which will leave an estimated 3 Gt CO_2 per year (~0.82 Gt C per year) of hard-to-abate emissions[34]. In offsetting these residual emissions, the LULUCF sector could significantly contribute to China's ambition. Under the continued forestation scenario, our simulations estimate that direct land carbon removals from LULUCF (averaging −0.28 ± 0.02 Gt C yr^{-1}) could compensate for around 34 ± 3% of these hard-to-abate emissions (Table 1). Furthermore, by adding the indirect effects in managed forest (−0.07 ± 0.03 Gt C yr^{-1}) to the direct ones, the offset percentage increases to 43 ± 4%. However, we must insist that this inclusion of the indirect effects in the definition of carbon neutrality is incompatible with the notion of remaining carbon budgets, and precautions must be taken when doing so[13].

The accelerated forestation scenario markedly increases total carbon removal until 2060, achieving a reduction of about half the hard-to-abate emissions (50 ± 5%; Table 1), and surpassing the continued forestation scenario in the short-term. Yet, due to finite forestation space (317 Mha, Fig. 2a), this initial benefit levels off after 2060, with both the accelerated (−25.4 ± 2.4 Gt C) and continued (−26.0 ± 2.5 Gt C) scenarios eventually reaching similar cumulative carbon removals in 2100 as all available land is exhausted. Conversely, adhering strictly to pledged forestation targets significantly reduces the emissions offset to 24 ± 4% in 2060 and decreases the overall carbon removal to about two-thirds of its full potential (−17.7 ± 2.0 Gt C) for the period 2019–2100, highlighting the crucial need for ongoing forestation efforts beyond initial commitments.

Moreover, if newly planted forests were more heavily exploited for wood harvest (following SSP5-8.5, Supplementary Fig. 4), the direct carbon removal would be reduced by about 0.02 Gt C yr^{-1} in 2060. This reduction occurs because the accelerated transfer of carbon from forests to wood products shortens the system's carbon retention time, diminishing long-term carbon sequestration. In the extreme case where forests are heavily exploited for wood production, the capacity for carbon capture could be entirely lost unless the lifespan of wood products is also extended. Long-lived wood products provide prolonged carbon storage, while short-lived products release carbon into the atmosphere more rapidly. In the context of a future bio-based society, maximizing the lifespan of wood products becomes crucial for enhancing carbon sequestration and mitigating climate change[35–37].

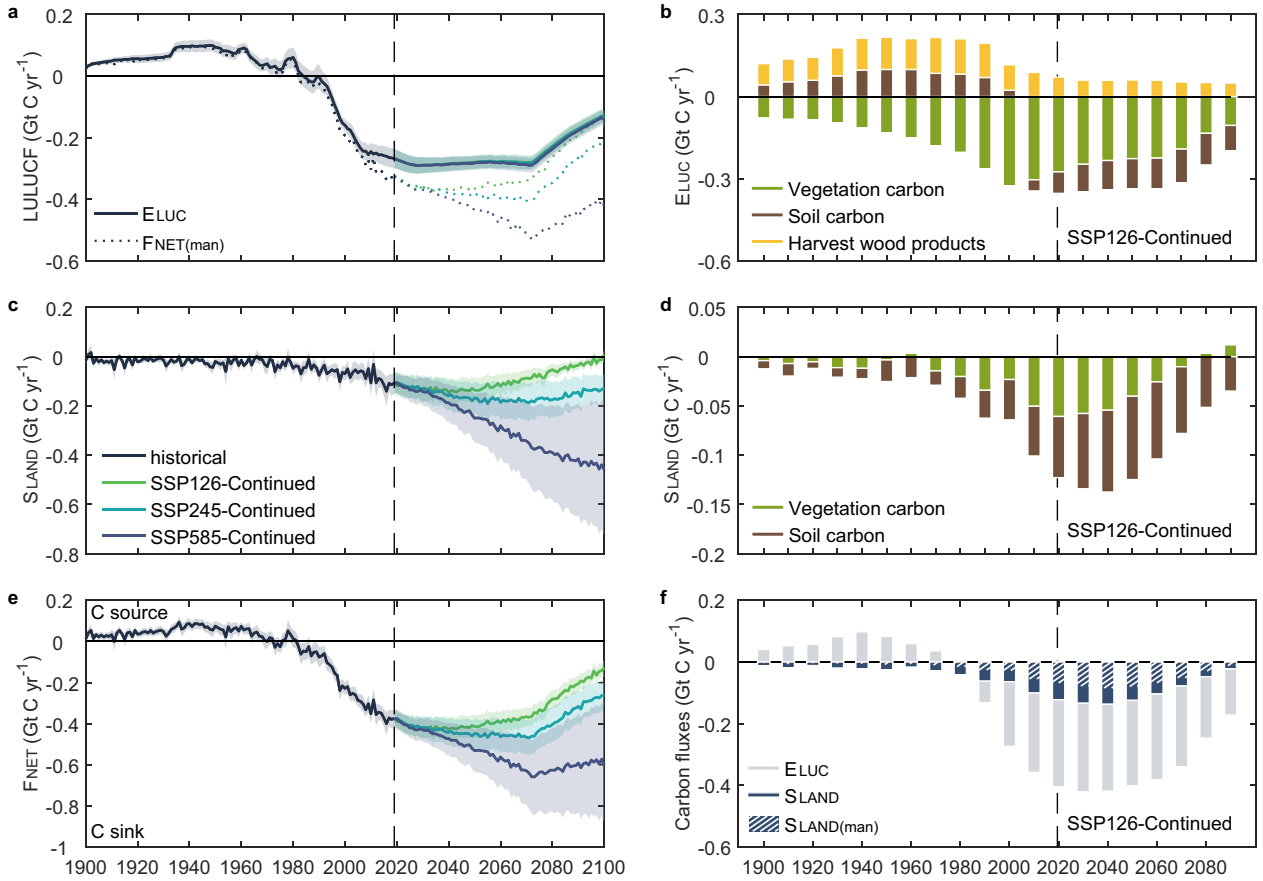

Fig. 3 | Historical and future trajectories of China's land carbon dynamics. **a**, **c**, **e** Annual land carbon fluxes: Land Use, Land-Use Change, and Forestry (LULUCF) fluxes based on different definitions (E_{LUC} and $F_{NET(man)}$), indirect effects resulting from environmental changes (S_{LAND}), and the combined total of direct and indirect effects (i.e., the net land carbon sink, $F_{NET} = E_{LUC} + S_{LAND}$). Results are shown for three climate change scenarios (that is, SSP1-2.6, SSP2-4.5, and SSP5-8.5) with a continued forestation land-use change scenario (Methods). The shaded areas represent the weighted standard deviation from a constrained Monte Carlo ensemble of 1000 elements. **b**, **d**, **f** Detailed breakdown of E_{LUC}, S_{LAND}, and F_{NET} under the SSP126-Continued scenario, delineating the contributions from vegetation, soils, and harvested wood products for E_{LUC} and S_{LAND}, and from E_{LUC} and S_{LAND} for F_{NET}. Data are presented as decadal averages from 1900s to 2090s for clarity.

We also explored different strategies for allocating annual forestation area (Fig. 2b; see Methods for details). By prioritizing forestation in regions based on their forest carbon density, high or low, we can bracket the range of uncertainties in annual carbon sequestration, despite reaching the same cumulative level by century's end (Fig. 2b and Table 1). The contribution of the LULUCF sector can, therefore, be effectively managed and shaped by strategic decisions regarding the timing and location of forestation efforts, but remains ultimately bounded.

Discussion

While China's climate mitigation commitments, such as those outlined in its NDC, specify targets for forestation, comprehensive quantification of the corresponding carbon removal potential demands investigation. Our study fills this critical gap by utilizing the OSCAR-China model to convert these forestation targets into explicit carbon sequestration estimates for the LULUCF sector. However, the mitigation potential from forestation should not be overstated, and anthropogenic appropriation of the natural land sink should be done with extreme care. First, the efficacy of expanding forest areas for enhancing direct carbon sequestration is limited in time: once the available area suitable for forestation is fully utilized, the carbon sink will inexorably diminish (Fig. 2). Second, the effectiveness of indirect carbon removal will likely weaken over time as global mitigation efforts progress, due to its dependence on atmospheric CO_2 levels, as well as deleterious climate impacts and increasing nutrients limitations[4,13,38,39]. Therefore, the carbon removal potential of the LULUCF sector is inherently limited but non-negligible.

Moreover, our estimate primarily centers on the potential of LULUCF under fairly optimistic assumptions. However, this potential could be significantly affected by various external factors that are not fully considered here. These include disturbances such as extreme wildfires and pest infestations, along with other climate extremes like droughts and heat waves, which can severely disrupt forest growth and reduce carbon sequestration capacity[40–42]. For instance, while our model accounts for wildfires by simulating fire intensity based on climate conditions and CO_2 levels, it does not fully capture extreme wildfire events or human interventions, such as efforts to limit and control natural wildfire[11,12]. In addition to natural disturbances, socioeconomic factors, such as forest management practices (e.g., wood harvest, thinning, and selective logging) and land use policies, are critical in determining the actual achievable sink level. However, in the current model, only wood harvest has been explicitly accounted for, while other factors—such as competition for land with food production, economic incentives for afforestation, and sustainable land management practices—are not yet integrated[43,44]. Consequently, while our findings provide a foundational understanding of the LULUCF sector's potential, they are likely optimistic. Future studies would benefit from integrating these broader considerations to provide refined estimates.

https://doi.org/10.1038/s41467-024-54846-2

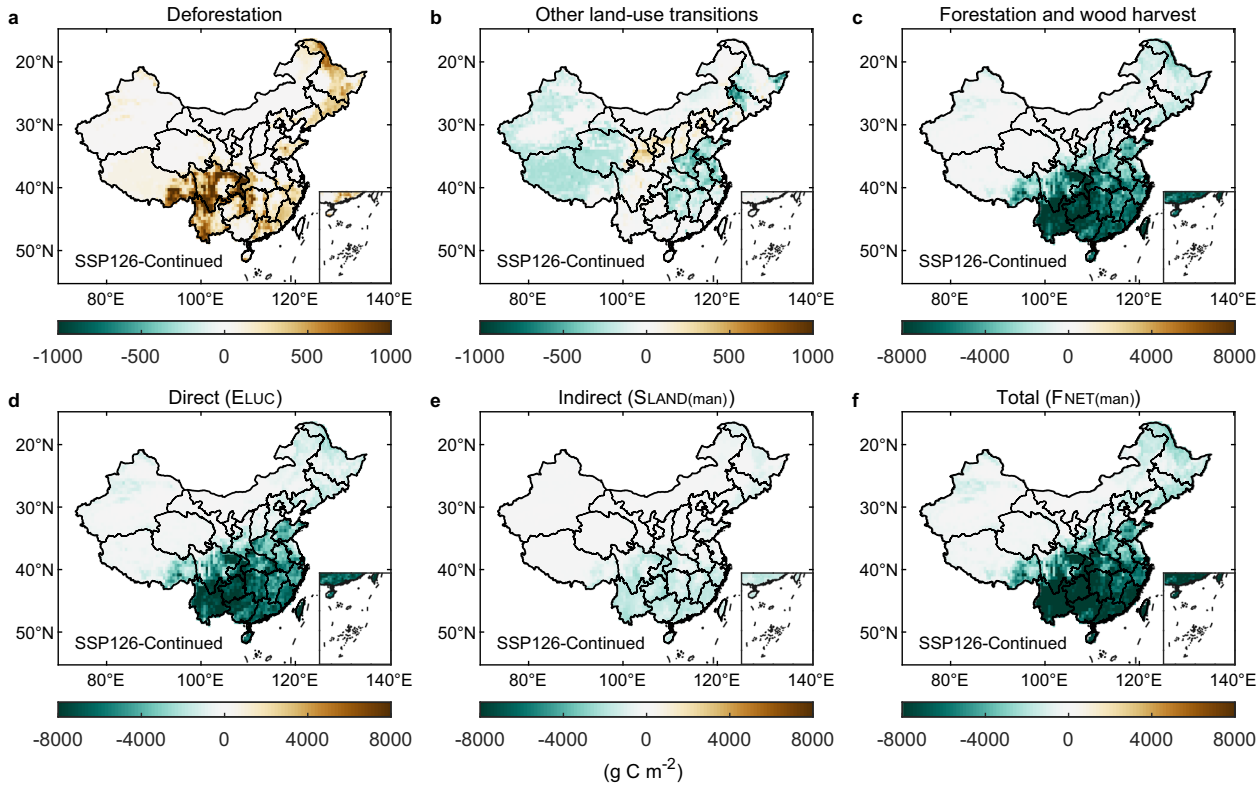

Fig. 4 | Land Use, Land-Use Change, and Forestry (LULUCF) carbon fluxes accumulated over 2019-2100, with detailed breakdown by key land-use change activities and by processes. a–c Cumulative LULUCF by direct effects attributed to forestation, deforestation, and other land use change transitions under the SSP126-Continued scenario, respectively. **d–f** Cumulative LULUCF by direct effects (E_{LUC}), indirect effects ($S_{LAND(man)}$), and total effects ($F_{NET(man)}$) under the same scenario, respectively.

In summary, our results highlight the opportunity for climate change mitigation through LULUCF policies, but also that this role should be viewed as complementary and only providing time for deep decarbonization of other sectors[25]. While our various scenarios provide an overview of the potential of forestation, they do not replace the nuanced, localized planning required for specific forestation initiatives[45–47]. This is particularly pertinent given the diverse ecological, climatic, and socio-economic contexts across regions. Furthermore, considering the definition gaps in the accounting of land-based carbon fluxes, it is imperative that national experts and scientists come together to enhance the processes of monitoring, reporting, and verifying the carbon fluxes of the LULUCF sector[13,48].

Methods

Overview of the OSCAR model

OSCAR is a reduced-complexity Earth system model designed to mimic the behavior of more sophisticated models, facilitating analysis of long-term climate policies and carbon budgets[12,49–52]. The standard version of OSCAR does not operate on a grid scale; instead, it functions at the regional and country levels. Despite this, it maintains a level of flexibility, allowing the scale to be adjusted in response to specific research needs. Its streamlined complexity reduces computing requirements, thus making it an efficient tool for these types of investigations. In terms of calibration, the preindustrial steady-state parameters of the land carbon cycle are based on TRENDYv7 models[53,54], eliminating the need for spin-up. The transient response of land ecosystems to changes in climate and CO_2 concentration is calibrated on the CMIP5 simulations[55]. OSCAR is meant to be used within a probabilistic framework: simulations with a large range of parameters in a Monte Carlo ensemble, the results of which can then be constrained with observation data[12].

OSCAR-China model

We expanded OSCAR v3.2 into a grid-based version for China, herein referred to as OSCAR-China. Our modified version functions at a $0.5° \times 0.5°$ scale, thereby providing a spatially explicit representation of localized land use and land-cover changes and their corresponding effects on the carbon cycle. Given the limitations of the TRENDYv7 model ensemble in providing detailed carbon stocks and fluxes for each plant functional type, direct calibration of steady-state parameters for China at the $0.5° \times 0.5°$ scale is not feasible. Instead, we adopted an approach grounded on Equation A45 from ref. 12. This involves categorizing China into seven large geographical regions (Supplementary Fig. 5), and then separately estimating steady-state parameters for each of these regions. Subsequently, these regionally derived parameters are applied to all grid points within their corresponding regions. In this study, we leverage the OSCAR-China model in an "offline" mode to more accurately simulate land carbon dynamics in China. In this context, "offline" refers to the model being driven by external observational inputs, such as CO_2 concentrations and climate data, rather than simulating these drivers internally within the model. More details about the experimental setups are provided in the following sections.

Historical experimental setup

We initiated the OSCAR-China model in 1800 but only reported carbon fluxes from 1900 to 2018 to account for the legacy effect of land-use history on current carbon dynamics. The simulation is driven by two primary types of forcing data: environmental changes (atmospheric CO_2 concentrations, temperature and precipitation), and land-use change perturbations (land cover change, wood harvest and shifting cultivation). Atmospheric CO_2 concentrations are taken directly from the GCB protocol[56]. Observation-based temperature and precipitation

data over the 1901–2018 period are sourced from CRU-TS v4.06[57], with pre-1901 values estimated using the 1901–1920 average as a pre-industrial baseline.

For a historical land cover change, we rely on the Yu22 dataset, a recent reconstruction with corrected biases by integrating multiple sources of inventories and observations[9]. This dataset categorizes land into five biomes: forest, cropland, grass, shrub, and wetland. To align this dataset with the biomes endogenously modeled in OSCAR-China (forest, non-forest, cropland, pasture, and urban), a categorical realignment is performed. Specifically, forest and cropland in Yu22 correspond directly to OSCAR-China, while shrubs and wetlands are reclassified as non-forest. Grass in Yu22 is divided into non-forest and pasture using HYDE3.2. The urban category, absent in Yu22, is supplemented from LUH2-GCB2019[58]. To maintain consistency, any increase in urban area is offset by a corresponding decrease in the non-forest category, ensuring biome area fractions sum to 100% in each grid cell. Due to the lack of pre-1900 land cover change data, we use a back-casting approach with LUH2-GCB2019's transition matrix and the 1900 land cover data to reconstruct changes from 1800 to 1899. Our method's robustness is supported by the close alignment of our 1800 forest area estimate with an independent dataset[59]. For a concise overview of biome area changes in China, see Supplementary Fig. 6. Furthermore, given that shifting cultivation primarily occurs between the latitudes of 33°N and 33°S, we assumed its absence in China and set this factor to zero. Wood harvest data are based on the Global Forest Resources Assessment (FRA) national-level data and spatially allocated according to the distribution of primary and secondary forests in China as reported by LUH2-GCB2019.

To meet the specific needs of OSCAR-China, it was essential to develop a transition matrix for land cover change. We, therefore, assumed that the area increase of one biome is proportionally distributed across other biomes experiencing area decrease within the same grid cell and year, based on their respective shares of total area decrease (proportional allocation; Supplementary Fig. 7). Note that by construction, this approach only provides net land cover transitions without gross gains and losses in the same grid cell and a given year.

Future scenario design

To conduct future simulations from 2019 to 2100, OSCAR-China requires the same type of input data as those utilized in historical simulations. For this study, we develop future projections of carbon dynamics by integrating three climate change scenarios with three land-use change scenarios.

Future temperature and precipitation time series under SSP1-2.6, SSP2-4.5, and SSP5-8.5 are taken directly from the database employed in the CMIP6 project, as the multi-model average of 31 models (Supplementary Table 3). To combine with historical data, we apply an additive adjustment factor (offset) to temperature data and a multiplicative adjustment factor (scaling) to precipitation data, using the average values from 2000 to 2018 as reference (Supplementary Fig. 8a, b). All CMIP6 outputs are re-gridded to 0.5° spatial resolution for China using a first-order conservative remapping scheme, as implemented by climate data operators (https://code.zmaw.de/projects/cdo). As for future atmospheric CO_2 concentrations under varying SSPs (Supplementary Fig. 8c), we rely on data provided by ref. 60.

In developing future land-use change scenarios, our approach first focuses on constructing forest area change scenarios aligned with national targets. These involve three forest expansion trajectories and corresponding spatial allocation strategies, detailed in their respective sections. Following the establishment of forest area change scenarios, we supplement the model with data for other biome area changes and wood harvest information using the LUH2 v2f dataset under the sustainable scenario SSP1-2.6[61]. This choice of scenario is in line with the national forestation targets in China. This step involves adapting data for cropland and urban areas directly from LUH2 v2f, while changes in pasture and non-forest areas are estimated based on their proportional representation within this dataset. To align the future projections of wood harvest and correct biases in cropland and urban areas between LUH v2f and historical data, an additive adjustment factor is used with the year 2018 as the reference point. Moreover, the expansion of forest areas could also potentially lead to an increase in wood harvest in the future. To account for this possibility, we also introduce the wood harvest from the LUH2 v2f SSP5-8.5 scenario into our analysis, which projects enhanced wood harvest in the future. This scenario provides a contrasting perspective to the SSP1-2.6, where forest will remain mostly unexploited, offering a comprehensive view of the potential outcomes stemming from China's national forestation targets (Supplementary Fig. 8d).

Forest expansion trajectories

Three distinct forest expansion trajectories are developed, each based on a combination of current national forestation targets (Supplementary Table 1), potential forest distribution, and different assumptions about policy implementation and ambition levels, offering a spectrum of possible futures for forest area expansion in China. To model the transition between different target years, a linear interpolation method is employed, ensuring a smooth and gradual change in forest area over time. See details in Supplementary Table 4.

Spatial allocation strategies of forestation

In our study, we have devised three distinct strategies to prioritize and allocate annual forestation opportunities. Our default approach, the sustainable potential-based strategy, involves a gradual and equitable distribution of forestation efforts across all regions. This strategy is guided by the available potential forestation space, promoting continuous forestation to ensure ecological balance and sustainability.

In addition to this, we have formulated two more targeted strategies, prioritizing forestation in regions with low or high-carbon density of forest ecosystems. These strategies are designed to bracket the ranges of uncertainty in future forestation efforts. The first, with a low-carbon density priority strategy (named "Low") allocates forestation space each year by prioritizing areas with lower carbon density first before moving to higher-density regions. Its goal is to prioritize ecological restoration in these regions, thereby enhancing carbon sequestration in areas that are currently less dense in forest carbon. Conversely, the high-carbon density priority strategy (named "High") directs forestation efforts to regions with higher carbon density first before moving to lower-density regions. This approach ensures that forestation efforts are strategically concentrated in areas with the greatest potential for immediate carbon sequestration.

In our study, we employ a clear nomenclature for various climate and land-use change scenarios, such as "SSP126-Continued", "SSP126-Continued-Low" and "SSP126-Continued-High". Note that unless explicitly stated otherwise within the main text, our study defaults to the sustainable potential-based strategy for forestation, with both "High" and "Low" scenarios used only for sensitivity analysis.

Potential forest distribution

We identify potential forest areas based on three datasets from ref. 25, which include predictions from a random-forest model, the World Resources Institute, and the ORCHIDEE dynamic global vegetation model. We focus on areas consistently classified as potential forests across all three sources, ensuring reliability by selecting their intersection. Two key constraints were applied in defining potential forest areas: (1) present-day forest area constraint: if the estimated potential forest area for a grid cell is smaller than its existing forest area in 2019, we adjust the potential area to equal the existing one; (2) non-forest and pasture area are hard constraints. Considering the intensive use

and socio-economic value of cropland and urban areas, the potential for converting these lands to forests is limited. Therefore, the potential opportunity for forest area increase is capped by the available non-forest and pasture area within the grid cell. If the increase in forest area exceeds the total available non-forest and pasture land, we adjust the potential forest area to the combined area of the existing forest, non-forest land, and pasture land. This ensures our projections align with practical land-use change possibilities. As a result, our analysis reveals that there is still an additional 98 Mha suitable for forestation (Supplementary Fig. 9), with a potential forest area of 317 Mha compared to the current 219 Mha in 2019.

Managed forest area changes

To track the managed forest area changes in China from 1900 to 2100, the following steps are taken. First, similar to the approach of ref. 62, we use a dataset (hereafter Han&Pot) that classifies forests in 2013 as either "intact" or "non-intact", interpreting "non-intact" as managed, to ascertain the proportion of managed to total forest area in China[63,64]. By applying this proportion, we identified the area of managed forests within the land-use change-forcing data for the corresponding year. This approach was chosen because the total forest area in this dataset was found to be relatively lower than other sources (see Fig. 1c), making it necessary to use the proportion to more accurately represent the extent of managed forests. Note that for regions in the proportion map where forest data is absent, we assume that the proportion of managed forest is the same as the nearest available value.

Due to insufficient historical data, we then assume that all forest area gains from 1900 to 2100 were in managed forests. For forest losses, our model differentiates between two periods: losses before 1980 are assumed to come from unmanaged forests, reflecting less active forest management at the time. Post-1980 losses are attributed to managed forests, coinciding with the onset of major forest restoration projects around the 1980s. This allowed us to extrapolate changes in managed forests backward to 1900 and forward to 2100, using the 2013 data as a starting point. The resulting changes in both total and managed forest areas are depicted in Supplementary Fig. 10.

Constrained Monte Carlo ensemble

We run one historical experiment and various combinations of future scenarios, each relying on a Monte Carlo ensemble of 1000 biogeochemical parameterizations to address uncertainty. These parameterizations are selected at random and with an equal chance from a pool of potential parameter sets[12,65]. To constrain our simulation results, we utilize two observation-based benchmarks specific to China. The first is the net land carbon sink (F_{NET}) over the 2000 to 2019 period, reported as -0.30 ± 0.037 Gt C yr^{-1} [30] in the latest Regional Carbon Cycle Assessment and Processes report (RECCAP2)[31]. Note that lateral fluxes, not captured by the OSCAR-China model, are excluded from the F_{NET} benchmark. The second is the forest vegetation carbon stock (cVeg) from the 9th NFI, reported as 8.98 Gt C on a national scale for the period spanning 2014 to 2018[66]. The NFI's survey accuracy is over 90%, which suggests an inherent uncertainty of ~10%. To remain conservative, we double this figure to 20%, resulting in a standard deviation of 1.80 Gt C for the forest cVeg. For each simulation of the ensemble ($N = 1000$), we assign a weight w_1 based on its alignment with the F_{NET} benchmark, and a weight w_2 based on its alignment with the forest cVeg benchmark. All these weights are computed using the Gaussian function as Eqs. (1) and (2):

$$w_1(x) = \frac{1}{\sigma_{F_{NET}}\sqrt{2\pi}} \exp\left(-\frac{\left(x-\mu_{F_{NET}}\right)^2}{2{\sigma_{F_{NET}}}^2}\right) \quad (1)$$

$$w_2(x) = \frac{1}{\sigma_{cVeg}\sqrt{2\pi}} \exp\left(-\frac{\left(x-\mu_{cVeg}\right)^2}{2{\sigma_{cVeg}}^2}\right) \quad (2)$$

where μ and σ are the mean and standard deviation of the benchmarks, and x is the value of the corresponding variable for each simulation of the ensemble. Each Monte Carlo simulation is then assigned a final weight w_3 by normalizing the product of w_1 and w_2 across all simulations as shown in Eq. (3):

$$w_3 = \frac{w_1 \cdot w_2}{\sum_{i=1}^{N} w_{1,i} \cdot w_{2,i}} \quad (3)$$

This normalization ensures that the sum of weights w_3 over all simulations equals one, allowing them to be properly used as probability weights for calculating the weighted averages and standard deviations of the simulation outputs. All results provided are the ensuing constrained weighted averages and weighted standard deviations. In Supplementary Fig. 11, we present the Monte Carlo distributions for key variables (E_{LUC}, F_{NET}, S_{LAND}) in the OSCAR-China model, both before and after applying the constraint.

Calculation of the loss of additional sink capacity

Our model is capable of calculating the "loss of additional sink capacity" (LASC), which is defined as the difference between the actual land sink under changing land cover and the hypothetical land sink that would have existed under preindustrial land cover[11]. This term, inherently included in E_{LUC} calculations from dynamic global vegetation models, is absent from bookkeeping models and inventories due to its counterfactual nature and its enduring presence after LULUCF activities have ceased. In China, LASC has been a small but consistent source of emissions from 1900 to 2018, primarily due to deforestation since preindustrial times. It is then projected to act as a carbon sink, owing to increased forestation activities, as detailed in Supplementary Fig. 12.

The NGHGI LULUCF database

The NGHGIs submitted by parties to the United Nations Framework Convention on Climate Change (UNFCCC) provide data on greenhouse gas emissions and removals, with the LULUCF sector as a key component conceptually aligned with the $F_{NET(man)}$ definition used in our paper. In the case of China, a non-Annex I country, NGHGI data are reported intermittently through National Communications and Biennial Updated Reports. The NGHGI LULUCF data for China collected in our study includes the years 1994, 2005, 2010, 2012, 2014, 2017, and 2018 (Supplementary Table 5). To address gaps in reporting, we applied linear interpolation to estimate missing values and generated a continuous dataset for 1994–2018. This dataset was then used to calculate multi-year averages, as shown in Fig. 1b.

The FAOSTAT LULUCF database

The FAOSTAT LULUCF database, managed by FAO, provides globally standardized data on LULUCF. Its estimates are based on forest resources data reported by countries, including inputs from the FRA on biomass stocks and forest area. Unlike NGHGIs, FAOSTAT uses a consistent methodology across countries, offering an independent perspective on LULUCF emissions and removals.

Integrated assessment models

In this study, we show results from IAMs drawn from the IIASA AR6 Scenarios Database. The IAM-generated estimates of E_{LUC} were informed by the database's Agriculture, Forestry, and Other Land Use (AFOLU) variables. Since, by construction, CO_2 emissions from agriculture are zero in the database, this AFOLU variable corresponds to

the E_{LUC} of our study. Moreover, we derive our IAM mean from an aggregation of available model data over the period of 2005–2100 from 1685 scenarios for China.

Bookkeeping models used in Global Carbon Budget assessment
In our study, we incorporate results from three prominent bookkeeping models used in the GCB2023[67]: H&C[22], BLUE[20], and OSCAR-GCB[12]. These models have been widely adopted in the field of carbon cycle research and provide comprehensive, scientifically robust insights into terrestrial carbon emissions. Data for all three models are retrieved from the supplementary information provided in the GCB2023. Specific data related to peatland fires in China were sourced directly from the BLUE team.

Data availability
The input data used for the OSCAR-China model, as well as the resulting output data, are available at Zenodo (https://zenodo.org/records/11182160).

Code availability
The main scripts for running the OSCAR-China model are openly accessible on GitHub (https://github.com/yuehe1313/OSCAR-China). Additionally, the source code for the foundational version of OSCAR can be accessed at https://github.com/tgasser/OSCAR.

References

1. Meinshausen, M. et al. Realization of Paris Agreement pledges may limit warming just below 2 °C. *Nature* **604**, 304–309 (2022).
2. UNFCCC. Nationally determined contributions under the paris agreement: revised note by the secretariat. United Nations Framework Convention on Climate Change (2021).
3. Liu, Z. et al. Challenges and opportunities for carbon neutrality in China. *Nat. Rev. Earth Environ.* **3**, 141–155 (2021).
4. Piao, S., Yue, C., Ding, J. & Guo, Z. Perspectives on the role of terrestrial ecosystems in the 'carbon neutrality' strategy. *Sci. China Earth Sci.* **65**, 1178–1186 (2022).
5. Griscom, B. W. et al. Natural climate solutions. *Proc. Natl Acad. Sci. USA* **114**, 11645–11650 (2017).
6. Bryan, B. A. et al. China's response to a national land-system sustainability emergency. *Nature* **559**, 193–204 (2018).
7. Chen, C. et al. China and India lead in greening of the world through land-use management. *Nat. Sustain.* **2**, 122–129 (2019).
8. Lu, F. et al. Effects of national ecological restoration projects on carbon sequestration in China from 2001 to 2010. *Proc. Natl. Acad. Sci. Usa.* **115**, 4039–4044 (2018).
9. Yu, Z. et al. Forest expansion dominates China's land carbon sink since 1980. *Nat. Commun.* **13**, 5374 (2022).
10. Bastos, A. et al. Comparison of uncertainties in land-use change fluxes from bookkeeping model parameterisation. *Earth Syst. Dyn.* **12**, 745–762 (2021).
11. Gasser, T. & Ciais, P. A theoretical framework for the net land-to-atmosphere CO_2 flux and its implications in the definition of 'emissions from land-use change'. *Earth Syst. Dyn.* **4**, 171–186 (2013).
12. Gasser, T. et al. Historical CO_2 emissions from land use and land cover change and their uncertainty. *Biogeosciences* **17**, 4075–4101 (2020).
13. Gidden, M. J. et al. Aligning climate scenarios to emissions inventories shifts global benchmarks. *Nature* **624**, 102–108 (2023).
14. Grassi, G. et al. Reconciling global-model estimates and country reporting of anthropogenic forest CO_2 sinks. *Nat. Clim. Chang.* **8**, 914–920 (2018).
15. Pongratz, J., Reick, C. H., Houghton, R. A. & House, J. I. Terminology as a key uncertainty in net land use and land cover change carbon flux estimates. *Earth Syst. Dyn.* **5**, 177–195 (2014).
16. Schwingshackl, C. et al. Differences in land-based mitigation estimates reconciled by separating natural and land. *One Earth* **5**, 1367–1376 (2022).
17. Rosan, T. M. et al. A multi-data assessment of land use and land cover emissions from Brazil during 2000-2019. *Environ. Res. Lett.* **16**, 074004 (2021).
18. Yue, C., Ciais, P. & Li, W. Smaller global and regional carbon emissions from gross land use change when considering sub-grid secondary land cohorts in a global dynamic vegetation model. *Biogeosciences* **15**, 1185–1201 (2018).
19. Houghton, R. A. et al. Carbon emissions from land use and land-cover change. *Biogeosciences* **9**, 5125–5142 (2012).
20. Hansis, E., Davis, S. J. & Pongratz, J. Relevance of methodological choices for accounting of land use change carbon fluxes. *Glob. Biogeochem. Cycles* **29**, 1230–1246 (2015).
21. Grassi, G. et al. Carbon fluxes from land 2000–2020: bringing clarity to countries' reporting. *Earth Syst. Sci. Data* **14**, 4643–4666 (2022).
22. Houghton, R. A. & Castanho, A. Annual emissions of carbon from land use, land-use change, and forestry from 1850 to 2020. *Earth Syst. Sci. Data* **15**, 2025–2054 (2023).
23. Zhang, G. et al. Regional differences of lake evolution across China during 1960s–2015 and its natural and anthropogenic causes. *Remote Sens. Environ.* **221**, 386–404 (2019).
24. He, N. et al. Vegetation carbon sequestration in Chinese forests from 2010 to 2050. *Glob. Chang. Biol.* **23**, 1575–1584 (2017).
25. Xu, H., Yue, C., Zhang, Y., Liu, D. & Piao, S. Forestation at the right time with the right species can generate persistent carbon benefits in China. *Proc. Natl Acad. Sci. USA* **120**, e2304988120 (2023).
26. Shang, R. et al. China's current forest age structure will lead to weakened carbon sinks in the near future. *Innovation* **4**, 100515 (2023).
27. Yu, Z., You, W., Agathokleous, E., Zhou, G. & Liu, S. Forest management required for consistent carbon sink in China's forest plantations. *For. Ecosyst.* **8**, 54 (2021).
28. Zhang, C. et al. Sustained biomass carbon sequestration by China's forests from 2010 to 2050. *Forests* **9**, 689 (2018).
29. Huang, L., Liu, J., Shao, Q. & Xu, X. Carbon sequestration by forestation across China: past, present, and future. *Renew. Sustain. Energy Rev.* **16**, 1291–1299 (2012).
30. Wang, X. et al. The greenhouse gas budget for China's terrestrial ecosystems. *Natl Sci. Rev.* **10**, 10–12 (2023).
31. Wang, X. et al. The greenhouse gas budget of terrestrial ecosystems in East Asia since 2000. *Glob. Biogeochem. Cycles* **38**, e2023GB007865 (2024).
32. Quilcaille, Y., Gasser, T., Ciais, P. & Boucher, O. CMIP6 simulations with the compact Earth system model OSCAR v3.1. *Geosci. Model Dev.* **16**, 1129–1161 (2023).
33. Canadell, J. G. et al. Intergovernmental Panel on Climate Change (IPCC). Global carbon and other biogeochemical cycles and feedbacks. *In*: Climate change 2021: the physical science basis. Contribution of working group I to the sixth assessment report of the intergovernmental panel on climate change 673–816 (Cambridge University Press, 2021).
34. Yu, G., Hao, T. & Zhu, J. Discussion on action strategies of China's carbon peak and carbon neutrality. *Bull. Chin. Acad. Sci.* **37**, 423–434 (2022).
35. Hart, J. & Pomponi, F. More timber in construction: unanswered questions and future challenges. *Sustainability* **12**, 3473 (2020).
36. Habert, G. Fast-growing bio-based materials can heal the world. *Build. Cities* **4**, 6 (2021).
37. Peñaloza, D., Erlandsson, M. & Falk, A. Exploring the climate impact effects of increased use of bio-based materials in buildings. *Constr. Build. Mater.* **125**, 219–226 (2016).

38. Terrer, C. et al. Nitrogen and phosphorus constrain the CO_2 fertilization of global plant biomass. *Nat. Clim. Chang.* **9**, 684–689 (2019).
39. Walker, A. P. et al. Integrating the evidence for a terrestrial carbon sink caused by increasing atmospheric CO_2. *N. Phytol.* **229**, 2413–2445 (2021).
40. Anderegg, W. R. L. et al. Climate-driven risks to the climate mitigation potential of forests. *Science* **368**, eaaz7005 (2020).
41. Liu, Z. et al. Forest disturbance decreased in China from 1986 to 2020 despite regional variations. *Commun. Earth Environ.* **4**, 15 (2023).
42. Reichstein, M. et al. Climate extremes and the carbon cycle. *Nature* **500**, 287–295 (2013).
43. Fujimori, S. et al. Land-based climate change mitigation measures can affect agricultural markets and food security. *Nat. Food* **3**, 110–121 (2022).
44. Tong, X. et al. Forest management in southern China generates short term extensive carbon sequestration. *Nat. Commun.* **11**, 1–10 (2020).
45. Erbaugh, J. T. et al. Global forest restoration and the importance of prioritizing local communities. *Nat. Ecol. Evol.* **4**, 1472–1476 (2020).
46. Holl, K. D. & Brancalion, P. H. S. Tree planting is not a simple solution. *Science* **368**, 580–581 (2020).
47. Strassburg, B. B. N. et al. Strategic approaches to restoring ecosystems can triple conservation gains and halve costs. *Nat. Ecol. Evol.* **3**, 62–70 (2019).
48. Grassi, G. et al. Critical adjustment of land mitigation pathways for assessing countries' climate progress. *Nat. Clim. Chang.* **11**, 425–434 (2021).
49. Fu, B. et al. Short-lived climate forcers have long-term climate impacts via the carbon–climate feedback. *Nat. Clim. Chang.* **10**, 851–855 (2020).
50. Fu, B. et al. The contributions of individual countries and regions to the global radiative forcing. *Proc. Natl Acad. Sci.* **118**, e201821111 (2021).
51. Gasser, T. et al. Accounting for the climate–carbon feedback in emission metric. *Earth Syst. Dyn.* **8**, 235–253 (2017).
52. Li, B. et al. The contribution of China's emissions to global climate forcing. *Nature* **531**, 357–361 (2016).
53. Le Quéré, C. et al. Global carbon budget 2017. *Earth Syst. Sci. Data* **10**, 405–448 (2018).
54. Sitch, S. et al. Recent trends and drivers of regional sources and sinks of carbon dioxide. *Biogeosciences* **12**, 653–679 (2015).
55. Arora, V. K. et al. Carbon-concentration and carbon-climate feedbacks in CMIP5 earth system models. *J. Clim.* **26**, 5289–5314 (2013).
56. Friedlingstein, P. et al. Global carbon budget 2021. 1917–2005 (2022).
57. Harris, I., Jones, P. D., Osborn, T. J. & Lister, D. H. Updated high-resolution grids of monthly climatic observations–the CRU TS3. 10 dataset. *Int. J. Climatol.* **34**, 623–642 (2014).
58. Chini, L. P. et al. LUH2-GCB2019: land-use harmonization 2 update for the global carbon budget, 850–2019. ORNL DAAC, Oak Ridge, Tennessee, USA. (2021).
59. FAO. Global forest resources assessment 2020: Main report. Food & Agriculture Organization of the United Nations (2020).
60. Meinshausen, M. et al. The shared socio-economic pathway (SSP) greenhouse gas concentrations and their extensions to 2500. *Geosci. Model Dev.* **13**, 3571–3605 (2020).
61. Hurtt, G. C. et al. Harmonization of global land use change and management for the period 850-2100 (LUH2) for CMIP6. *Geosci. Model Dev.* **13**, 5425–5464 (2020).
62. Grassi, G. et al. Harmonising the land-use flux estimates of global models and national inventories for 2000–2020. *Earth Syst. Sci. Data* **15**, 1093–1114 (2023).
63. Hansen, M. C. et al. High-resolution global maps of 21st-century forest cover change. *Science* **342**, 850–853 (2013).
64. Potapov, P. et al. The last frontiers of wilderness: tracking loss of intact forest landscapes from 2000 to 2013. *Sci. Adv.* **3**, 2020–2022 (2017).
65. Gasser, T. et al. The compact earth system model OSCAR v2.2: description and first results. *Geosci. Model Dev.* **10**, 271–319 (2017).
66. SFGA (State Forestry and Grassland Administration). China Forest Resources Report 2014–2018. China Forestry Publishing House: Beijing, China. (2019).
67. Friedlingstein, P. et al. Global carbon budget 2023. *Earth Syst. Sci. Data* **15**, 5301–5369 (2023).

Acknowledgements

This study was supported by the Horizon Europe research and innovation program of the European Union, specifically the RESCUE project, grant agreement no. 101056939 (T.G.), and by the Horizon 2020 research and innovation program of the European Union, specifically the ESM2025—Earth System Models for the Future project, grant agreement no. 101003536 (T.G.).

Author contributions

S.P. and T.G. designed the research; Y.H. performed the research and wrote the original draft; and C.P., H.X., T.G., and S.P. reviewed and edited the paper.

Competing interests

The authors declare no competing interests.

Additional information

Supplementary information The online version contains supplementary material available at https://doi.org/10.1038/s41467-024-54846-2.

Correspondence and requests for materials should be addressed to Shilong Piao or Thomas Gasser.

Peer review information *Nature Communications* thanks Yumeng Wang, E.V. Gubiy and the other, anonymous, reviewer(s) for their contribution to the peer review of this work. A peer review file is available.